



UNIVERSITÉ
DE GENÈVE

Archive ouverte UNIGE

<https://archive-ouverte.unige.ch>

Article scientifique

Article

2018

Supplemental data

Open Access

This file is a(n) Supplemental data of:

Free space laser telecommunication through fog

Schimmel, Guillaume; Produit, Thomas; Mongin, Denis; Kasparian, Jérôme; Wolf, Jean-Pierre

This publication URL:

<https://archive-ouverte.unige.ch/unige:109626>

Publication DOI:

[10.1364/OPTICA.5.001338](https://doi.org/10.1364/OPTICA.5.001338)

© The author(s). This work is licensed under a Other Open Access license

<https://www.unige.ch/biblio/aou/fr/guide/info/references/licences/>

Free space laser telecommunication through fog: supplementary material

GUILLAUME SCHIMMEL,¹ THOMAS PRODUIT,¹ DENIS MONGIN,¹ JÉRÔME KASPARIAN,^{1,2} AND JEAN-PIERRE WOLF^{1,*}

¹Group of Applied Physics, University of Geneva, Chemin de Pinchat 22, 1211 Geneva 4, Switzerland

²Institute for Environmental Sciences, University of Geneva, bd Carl Vogt 66, 1211 Geneva 4, Switzerland

*Corresponding author: Jean-Pierre.Wolf@unige.ch

Published 18 October 2018

This document provides supplementary information to “Free space laser telecommunication through fogs and clouds,” <https://doi.org/10.1364/OPTICA.5.001338>. Here we describe the experimental setup used to analyze the droplet clearing process in clouds using ultrashort high intensity laser filaments. The cleared channel created is used for transmitting high bit rate telecom data at 1.55 μm . We also discuss the thermal lensing effect due to the filaments, which is experimentally observed on the telecom laser beam.

Materials and Methods. The experimental setup, as depicted in Figure S1, relies on propagating ultrashort laser pulses through an artificial cloud, contained in a chamber of adjustable length and created by a micrometric droplet generator in an open-ended tube. The Ti:Sa laser system delivers 30 fs-long 800 nm laser pulses of 5 mJ with an initial beam diameter of 1 cm, slightly focused in the cloud chamber with a 1 m focal-length lens to form 20 cm-long filaments. The repetition rate of the pulses can be tuned from 10 to 1000 Hz while maintaining a constant pulse energy.

The cloud properties are adjustable in the chamber through several parameters, such as the length of the chamber (i.e. the length of interaction with the laser), the incoming speed of the droplets (wind), their initial concentration and the droplet size distribution. The optical attenuation of the artificial cloud (up to 20 dB) allows to reach optical densities of real cloud in the 100 m range thickness (typical cloud conditions exhibit 10-100 dB/km attenuation). The optical density of the cloud is continuously probed by an auxiliary laser (CW, HeNe at 633 nm, not shown on Fig. S1) positioned 20 mm away from the filament region in the transverse direction. This particle density remained stable, excluding any influence from potential laser-induced condensation [1].

The data-carrier telecom laser is a low power, amplitude modulated, distributed feedback laser diode at 1.55 μm which is aligned to the filament in a counter-propagating configuration that facilitates its detection and the tuning of its focusing independently from the high-power laser. An optical system implemented on the beam path aims at focusing the beam at the position of the filament with an adjustable numerical aperture, allowing manipulating the overlap with the filament region. As proof of principle, data encoding is performed through a square amplitude modulation applied to the laser diode at a frequency up to 1 GHz, which exhibits

the 0-to-1 and the 1-to-0 transitions. After the focusing optical system, the telecom laser propagates through the filament region located inside the cloud chamber. Collected with a lens, the radiation is then spectrally filtered in order to reject the background radiation and the high intensity laser light - rejection is above 40 dB below 1.4 μm . The analysis of the transmitted signal is performed using a 5 GHz InGaAs photodiode and a 3 GHz oscilloscope.

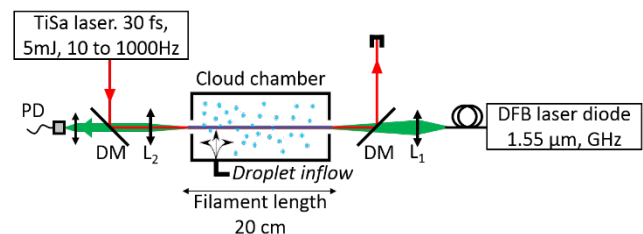


Fig. S1. Sketch of the experimental setup. The 800 nm beam path is in red; the counter-propagating 1550 nm beam in green. L1: focusing optical system; L2: 1 m focal length optic; PD: 5 GHz bandwidth, InGaAs photodiode; DM: dichroic mirror.

Defocusing effect of the telecom laser beam. Right after the filament shockwave, we observe a transmission drop of about 10 to 15%. These initial losses induced by the filament are illustrated in time on Figure S2, with and without cloud. The transmission gets back to maximum within a typical half time of 130 μs , slightly increased in the 1 kHz case. Such time scale indicates that these losses arise from the air refractive index gradient, associated with the heat deposited by the filament. This phenomenon has been previously described in the literature in the case of clean air [2-6]: the gas-depleted region exhibits a lower refractive index at the

center, which induces a defocusing effect on the data-carrier laser. This defocusing vanishes when the air density gradient disappears progressively, whereas the shockwave ejection of droplets remains efficient on about 40 times larger time-scales, due to the longer replenishment time. The fog-free average transmission is lower for laser filaments at 1 kHz as compared with 100 Hz (see also Fig. S3). It is consistent with the fact that successive pulses arrive before the transmission has completely recovered.

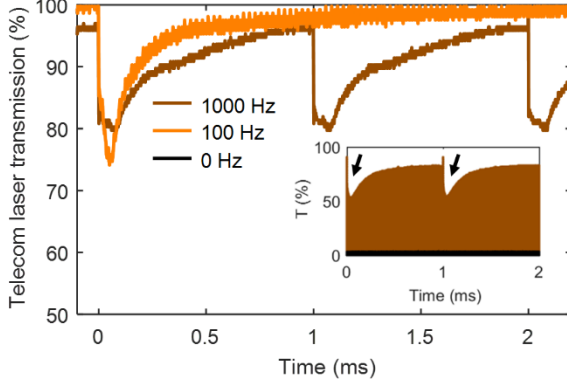


Fig. S2. Thermal defocusing effect induced by the filament on the counter-propagating beam, without fog for the cw case. Inset: transmission of the modulated laser (0.2 GHz) through fog (-12 dB transmission), with and without laser filaments; a comparable defocusing effect observed (arrows).

However, the transmission increase due to the fog clearing overrides the data carrier laser defocusing by the thermal effects, so that the overall effect of the filament is highly favorable to transmitting information with filaments repetition rates above 200 Hz. Conversely, it induces higher losses than fog scattering at repetition rates below 50 Hz. In this "blind window", no data should be sent by the transmitter nor expected by the detector. Similarly, when the repetition rate increases up to the point where the temporal separation between the pulses is close to the duration of the transient defocusing (i.e., above 5-10 kHz), one can expect that the transmission may decrease again. Therefore, repetition rates in the kHz range appear as an optimal condition.

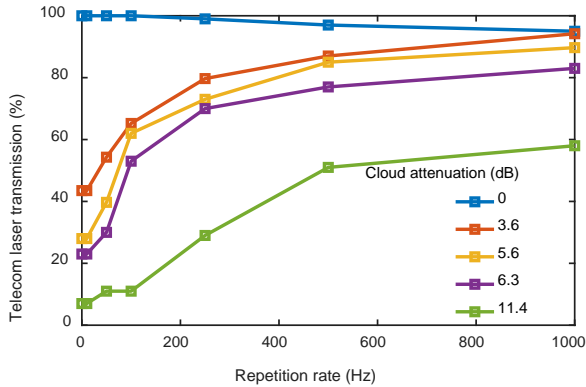


Fig. S3. Optical transmission of the data-carrier laser through the cloud chamber as a function of the high intensity laser repetition rate, displayed for several cloud optical attenuations (no fog corresponds to 0 dB attenuation without laser). The no-filament case corresponds to 0 Hz repetition rate.

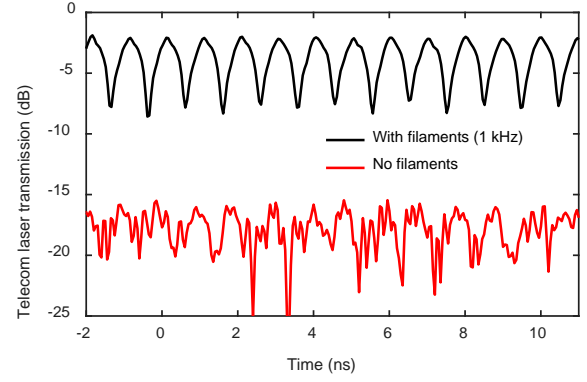


Fig. S4. Transmission of the 1 GHz amplitude modulated telecom laser through fog (-14 dB transmission) as a function of time, with and without laser filament (1 kHz) through fog. Detection of the square modulated signal is limited by the 3 GHz oscilloscope bandwidth.

Visualization 1. Side view of the data-carrier laser beam (visible cw 633 nm laser in this case) through fog with and without filament (1 kHz) and the associated scattering. The camera settings are fixed during the whole movie. The high intensity laser producing the filament is turned on from $t = 5$ s to $t = 13$ s. During this time interval, the 1 kHz sound produced by the shockwave is audible.

Visualization 2. Front view of the data-carrier laser beam (visible cw 633 nm laser in this case) transmitted through fog with and without filament (1 kHz). The camera settings are fixed during the whole movie. The high intensity laser producing the filament is turned on from $t = 2$ s to $t = 8$ s. During this time interval, the 1 kHz sound produced by the shockwave is audible.

References

1. S. Henin, Y. Petit, P. Rohwetter, K. Stelmazczyk, Z.Q. Hao, W.M. Nakaema, A. Vogel, T. Pohl, F. Schneider, J. Kasparian, K. Weber, L. Wöste, J.-P. Wolf, Field measurements suggest the mechanism of laser-assisted water condensation. *Nature communications*, 2, 456 (2011)
2. F. Vidal, D. Comtois, C.-Y. Chien, A. Desparois, B. L. Fontaine, T. W. Johnston, J. C. Kieffer, H. P. Mercure, H. Pepin, and F. A. Rizk, Modeling the triggering of streamers in air by ultrashort laser pulses, *IEEE Transactions on Plasma Science* 28, 418 (2000).
3. J. Yu, D. Mondelain, J. Kasparian, E. Salmon, S. Geffroy, C. Favre, V. Boutou, and J. P. Wolf, Sonographic probing of laser filaments in air, *Applied Optics* 42, 7117 (2003).
4. Y.-H. Cheng, J. K. Wahlstrand, N. Jhajj, and H. M. Milchberg, The effect of long timescale gas dynamics on femtosecond filamentation, *Optics Express* 21, 4740 (2013).
5. O. Lahav, L. Levi, I. Orr, R. A. Nemirovsky, J. Nemirovsky, I. Kaminer, M. Segev, and O. Cohen, Long-lived waveguides and sound-wave generation by laser filamentation, *Physical Review A* 90, 021801 (2014).
6. N. Jhajj, E. W. Rosenthal, R. Birnbaum, J. K. Wahlstrand, and H. M. Milchberg, Demonstration of long-lived high-power optical waveguides in air, *Physical Review X* 4, 011027 (2014).